COMPARISON OF GOCE DERIVED SATELLITE GLOBAL GRAVITY MODELS WITH EGM2008, THE OCTAS GEOID AND TERRESTRIAL GRAVITY DATA: CASE STUDY FOR NORWAY

M. Šprlák[(1)], C. Gerlach[(1), (2)], O. C. D. Omang[(3)], B. R. Pettersen[(1)]

[(1)] Institute for Mathematical Sciences and Technology, Norwegian University of Environmental and Life Sciences, Ås, Norway, michal.sprlak@umb.no, bjorn.pettersen@umb.no

[(2)] Commission for Geodesy and Glaciology, Bavarian Academy of Sciences and Humanities, Munich, Germany, gerlach@bek.badw.de

[(3)] Norwegian Mapping Authority, Geodetic Institute, N-3507, Hønefoss, Norway, Ove.Omang@statkart.no

ABSTRACT

Global gravity models composed of a set of spherical harmonic coefficients represent one of the most important products of the GOCE satellite gradiometry mission. These are of particular interest in many geo-scientific disciplines dealing with the Earth's gravity field. At present, four satellite-only global gravity models based on GOCE observations have been made available to the scientific community. Three of them have been determined by independent strategies using pure GOCE satellite-to-satellite tracking and satellite gravity gradiometry observations. The fourth model has been computed from a combination of GRACE and GOCE observations.

In this contribution, GOCE derived global gravity models are compared with EGM2008, the OCTAS geoid and terrestrial gravity anomalies. We restrict our numerical study to the territory bounding the continental part of Norway. Spherical harmonic expansions have been truncated at maximum degree and order 200 corresponding to a spatial resolution of 100km. Higher frequencies contained in the OCTAS geoid and in the terrestrial gravity anomalies have been removed by explicitly applying a low-pass filter on the data sets, or by removing the signal content of EGM2008 above degree 200.

1. INTRODUCTION

Planet Earth represents a complex dynamic system which may be described by geometrical and physical properties. Nowadays, geometrical positions can be determined by Global Navigation Satellite Systems (GNSS) with accuracy of some few millimeters. Such a level of accuracy is satisfactory for many industrial, commercial or even scientific purposes. On the other hand, physical properties of the Earth revealing important natural phenomena must not be neglected. One of the fundamental physical quantities is the Earth's gravity field. Especially functionals of the gravity potential in the form of a geoid and gravity anomalies are of particular interest.

According to the classical definition, the geoid represents an equipotential surface (almost) coinciding with the mean ocean surface, and which is also extended beneath the topographic masses on continents. In geodesy, precise knowledge of the geoid allows determination of orthometric heights by GNSS or realizing a global height reference system. In oceanography the geoid is of fundamental importance, because the deviations of the mean ocean surface from the geoid are a measure for ocean currents. In addition, the regional and global structure of the gravity field can be used for exploring the mass distribution in the Earth's crust and mantle, while temporal changes of the field give an indication of mass transport, e.g., for hydrological or glaciological applications.

Global representation of the gravity field in the form of a global gravity model (GGM) is usually based on spherical harmonics. From such a GGM any functional of the gravity potential may be evaluated. Several GGMs have been made available to the scientific community at the International Centre for Global Earth Models (ICGEM, see http://icgem.gfz-potsdam.de/ICGEM). Significant improvements in modeling the global gravity field have been made due to contributions of the satellite gravity missions CHAMP, GRACE and GOCE.

GOCE (Gravity field and steady-state Ocean Circulation Explorer) belongs to the core satellite missions of the European Space Agency [2]. Focusing on the static part of the global gravity field, GOCE is expected to provide a geoid model with an accuracy of 1 cm and gravity anomalies with an accuracy of 1 mGal at a spatial resolution of 100km. To achieve such a stimulating goal, satellite gravity gradiometry (SGG) has been realized onboard the low orbiting satellite. Three different approaches have been proposed to determine the spherical harmonic coefficients from GOCE. These are called the direct, the space-wise and the time-wise approach. GOCE-only GGMs from each of these three approaches have been provided to the user community. In addition there is one combined GOCE-GRACE model.

In this study, all of these four models are compared with EGM2008, the regional OCTAS geoid and terrestrial gravity anomalies. In chapter 2, the different datasets are discussed. In chapter 3, geoidal surfaces are compared. Similarly, gravity anomalies are compared in chapter 4. In the numerical experiments, we restrict

Proc. of '4th International GOCE User Workshop', Munich, Germany
31 March – 1 April 2011 (ESA SP-696, July 2011)

ourselves to the territory bounding the continental part of Norway and most of Fennoscandia. Spherical harmonic expansions have been truncated at maximum degree and order 200, corresponding to a spatial resolution of 100km. Higher frequencies of the OCTAS geoid and terrestrial gravity anomalies have been removed by two approaches. In the first approach, we subtract the higher frequencies (above degree 200) computed from EGM2008. In the second approach a low-pass filter is explicitly applied to the regional datasets. Making use of the Fast Fourier transform (FFT), this low-pass filtering is performed in the frequency domain.

2. DESCRIPTION OF INPUT DATASETS

A set of spherical harmonic coefficients available up to a finite degree and order of the spherical harmonic expansion forms a GGM. It allows evaluating arbitrary functional of the gravity potential on the surface of the Earth or in outer space. The spatial resolution of the evaluated functional is given by the maximum degree and order of the spherical harmonic coefficients. For the analysis of GOCE gradiometry, three independent approaches have been proposed, i.e. direct numerical, space-wise and time-wise. The direct numerical method has been applied in [1] combining precise science orbit positions and SGG observations. The corresponding model is complete up to degree and order 240. Migliaccio et al. [4] used satellite-to-satellite tracking (SST) and SGG observations in space-wise method, i.e. a multi-step collocation procedure, to determine GGM up to degree and order 210. Pail et al. [6] combined SST and SGG observations by the time-wise approach. In this manner, spherical harmonic coefficients up to degree and order 224 have been obtained. According to the applied approach, these three models will be denoted GOCE_DIR, GOCE_SPW and GOCE_TIM, respectively. Besides these pure GOCE-based models, Pail et al. [7] have published a first combination of GRACE and GOCE observations, the GOCO01S GGM. Its spherical harmonic coefficients are available up to degree and order 224. As a measure of the quality of the models, the formal standard deviations can be used. In Fig. 1, the cumulative error degree variances of geoid heights are illustrated. Evidently, GOCO01S model is superior at low frequencies. However, at degree and order 200, we can expect the same order of accuracy in geoidal heights for all models (ranging between 0.06m to 0.11m). Supposing the same degree and order, we can expect the accuracy of gravity anomalies to range between 1.8 to 3.5 mGal.

For validation purposes, when one makes sure that the measurement process, error estimation and calibration have been performed well [3], existing independent data or knowledge about the Earth's gravity field is used. In this study, we decided to perform a comparison of the GOCE derived models with the state-of-the-art global combination model EGM2008 [8]. In addition, the OCTAS (Ocean Circulation and Transport between the north Atlantic and the arctic Sea) geoid and mean free-air gravity anomalies, see [5], available in the test area have been used. The OCTAS geoid represents a high resolution gravimetric geoid model covering the north Atlantic, the Arctic Sea and Fennoscandia. To be precise, OCTAS is a quasigeoid rather than a geoid. OCTAS and a low-resolution geoid up to degree and order 200 are illustrated in Fig. 2. Over the continental part of Norway and most of Fennoscandia, linear trend of the geoidal surface in the longitudinal direction is dominating. Free-air block mean values of 5' × 5' terrestrial gravity anomalies used for validation purposes have been generated on the surface of the geoid by collocation. For this purpose, marine and terrestrial gravity data from the database of the Nordic Geodetic Commission (NKG) has been compiled. Mean free-air and low-degree gravity anomalies up to degree and order 200 are illustrated in Fig. 3. Unlike in case of the geoid, correlation of gravity anomalies with topography can be observed.

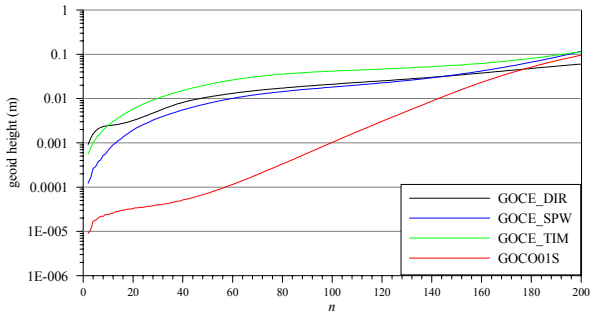

Figure 1: Cumulative error degree variances for geoid height

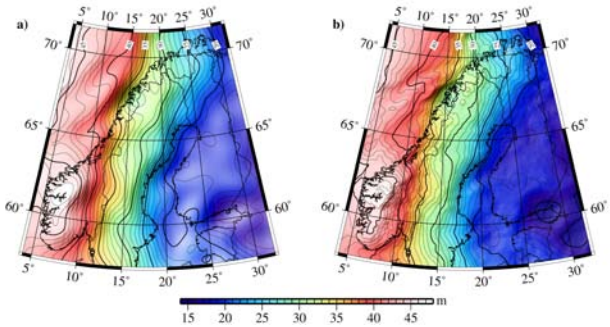

Figure 2: Geoid over continental part of Norway: a) Low-degree geoid computed from GOCE_DIR GGM up to degree and order 200, b) High-resolution OCTAS geoid

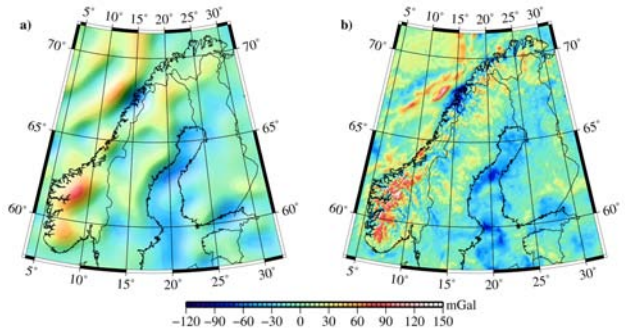

Figure 3: Gravity anomalies over continental part of Norway: a) Low-degree gravity anomalies computed from GOCE_DIR GGM up to degree and order 200, b) Mean gravity anomalies

3. COMPARISON OF GEOIDAL SURFACES

In the first numerical experiment, we compare geoidal surfaces computed from GOCE_DIR, GOCE_SPW, GOCE_TIM and GOCO01S as well as the OCTAS geoid to EGM2008. We have chosen a test area in the domain $\varphi \in \langle 57.5°, 71.5° \rangle$ and $\lambda \in \langle 4°, 32° \rangle$ bounding the continental part of Norway and most of Fennoscandia. To preserve the same spatial resolution of all geoidal surfaces, only spherical harmonic coefficients up to degree and order 200 have been considered for all GGMs under study. Accordingly also the high resolution OCTAS geoid needs to be low-pass filtered. Here two approaches were used.

Firstly, the high frequencies in the spectral range from 201 up to 2190 have been computed from EGM2008 and subtracted from the OCTAS geoid. Tab. 1 shows the statistics of the differences of all of the geoids with respect to EGM2008. Evidently, the differences reach several decimeters for GOCE derived GGMs and the filtered OCTAS geoid. Standard deviation for the filtered OCTAS geoid reaches only 0.055m. In the case of GOCE derived GGMs, higher values of standard deviation may be observed reaching up to 0.102m for the GOCE_TIM model. All geoid models are only slightly biased within few millimeters as the corresponding mean values indicate.

The differences are depicted in Fig. 4 and Fig 5a. Apparently, local maxima and minima occur at the same locations for GOCE_SPW, GOCE_TIM and GOCO01S. In the case of GOCE_DIR, the amplitudes of local maxima and minima are reduced. In contrast to GOCE derived GGMs, we can see a high frequency behavior of differences implied by the filtered OCTAS geoid in Fig 5a.

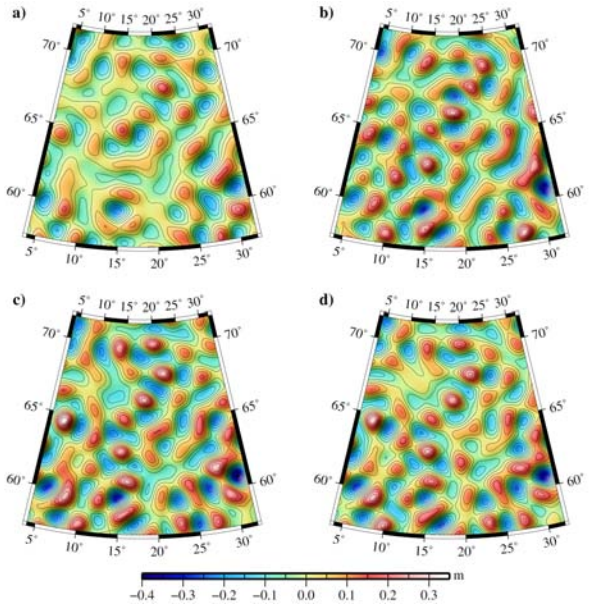

Figure 4: Comparison of geoidal surfaces computed by the GOCE derived GGMs with respect to EGM2008: a) GOCE_DIR, b) GOCE_SPW, c) GOCE_TIM, d) GOCO01S

Table 1: Statistics of differences between geoidal surfaces with respect to EGM2008 (high frequency part of the OCTAS geoid is removed by EGM2008)

Model	GOCE_DIR	GOCE_SPW	GOCE_TIM	GOCO01S	OCTAS
Min. (m)	-0.241	-0.367	-0.410	-0.374	-0.556
Max. (m)	0.209	0.291	0.343	0.299	0.430
Mean. (m)	-0.008	-0.003	-0.003	-0.001	0.005
Std. dev. (m)	0.067	0.093	0.102	0.092	0.055

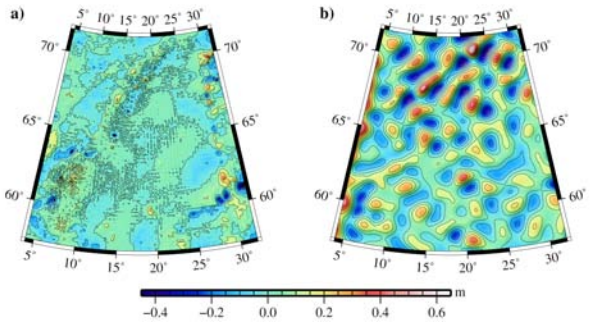

Figure 5: Comparison of the OCTAS geoid with respect to EGM2008: a) Removing of high-frequencies by EGM2008, b) Low-pass filtering in frequency domain

Supposing GOCO01S as reference, one obtains a better insight of relative differences between GOCE derived GGMs. The corresponding statistics are given in Tab. 2. The differences reach several centimeters with a mean value of only some few millimeters. GOCO01S seems to fit best to GOCE_TIM because both models are based on the time-wise approach. For GOCE_DIR and GOCE_SPW, standard deviations slightly above 0.06m have been reached. A graphical illustration is given in Fig. 6. Since only GOCE and GRACE data are involved in this comparison, the differences show a different structure than those with respect to EGM2008.

As an alternative, filtering of the OCTAS high resolution geoid was also carried out in the following way. First, we transformed the OCTAS geoid into the frequency domain by FFT. In the frequency domain a low-pass Butterworth filtering has been performed with a cut-off of 100km. After filtering, inverse FFT has been applied to obtain the low-pass filtered OCTAS geoid model back in the space domain. To preserve the same spatial resolution, the same filtering procedure has been applied for the geoid models evaluated from the GGMs. To avoid edge effects in the FFT, geoidal surfaces have been evaluated in a larger area and the final comparison has been performed in the test area mentioned above. Statistics of differences between low-pass filtered geoidal surfaces are given in Tab. 3. Here also a low-pass filtered version of EGM2008 was used as reference. Comparing these numbers with the statistics given in Tab.1, the minimum and maximum differences as well as the standard deviation decrease in case of the GOCE derived GGMs. However, for the OCTAS geoid, the standard deviation increased up to 0.139m with a small bias of 0.019m. An increase of the standard deviation is caused by the inaccuracies of the filtering method we proposed. We can also assume that our filtering procedure and the construction of frequency spectra is affected by the dominating linear trend of the geoid in the test area. The spatial behavior of the differences for the GOCE derived GGMs is of the same pattern as can we observe in Fig. 4 with reduced magnitudes of local minima and maxima. In Fig. 5b, the differences between the low-pass filtered OCTAS geoid and EGM2008 are illustrated. We can see only low frequency features without any correlations to topography. However, as it was already mentioned, differences contain also the accuracy of our filtering procedure which is on the level of several centimeters.

Table 2: Statistics of differences between geoidal surfaces with respect to GOCO01S

Model	GOCE_DIR	GOCE_SPW	GOCE_TIM
Min. (m)	-0.228	-0.196	-0.121
Max. (m)	0.242	0.237	0.131
Mean. (m)	-0.007	-0.002	-0.003
Std. dev. (m)	0.064	0.063	0.037

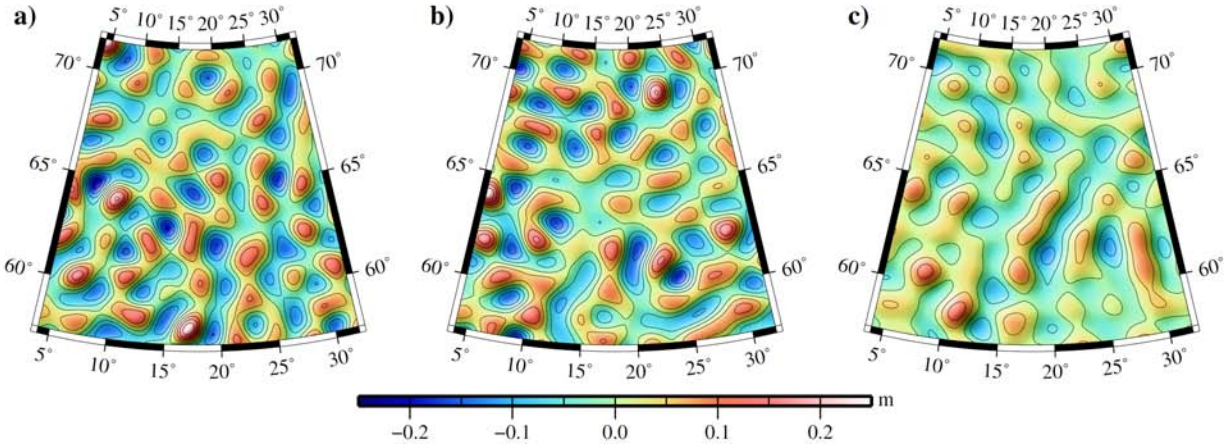

Figure 6: Comparison of geoidal surfaces computed by the GOCE derived GGMs with respect to GOCO01S: a) GOCE_DIR, b) GOCE_SPW, c) GOCE_TIM

Table 3: Statistics of differences between geoidal surfaces with respect to EGM2008 (geoidal surfaces filtered in frequency domain)

Model	GOCE_DIR	GOCE_SPW	GOCE_TIM	GOCO01S	OCTAS
Min. (m)	-0.196	-0.286	-0.314	-0.287	-0.455
Max. (m)	0.178	0.209	0.271	0.231	0.624
Mean. (m)	-0.007	-0.002	-0.003	0.000	0.019
Std. dev. (m)	0.057	0.073	0.080	0.072	0.139

4. COMPARISON OF GRAVITY ANOMALIES

In the second numerical experiment, we compare gravity anomalies from GOCE_DIR, GOCE_SPW, GOCE_TIM, GOCO01S, EGM2008 and terrestrial mean free-air gravity anomalies. The same test area in the range $\varphi \in \langle 57.5°, 71.5° \rangle$ and $\lambda \in \langle 4°, 32° \rangle$ has been considered. The same procedures as applied to the OCTAS geoid have been used for removing high frequency signal components from the terrestrial mean free-air gravity anomalies.

Let us first consider low-pass filtering by removing the high frequencies computed fom EGM2008 in the spectral range from 201 to 2190. Again gravity anomalies from the GGMs have been evaluated up to maximum degree and order 200. Tab. 4 shows the statistics of differences with respect to EGM2008. We can see that the differences reach several mGal in the case of GOCE derived GGMs. Analogous to the comparison of geoidal surfaces, the smallest standard deviation of 1.694mGal is achieved for GOCE_DIR while the highest standard deviation of 2.778mGal has been obtained for GOCE_TIM. Moreover, from the graphical illustration in Fig. 7 we can see the same pattern for each GOCE derived model as we observed for geoidal surfaces in Fig. 4. A significant distinction is evident in the case of terrestrial mean free-air gravity anomalies where differences reach even several tens of mGal. The graphical illustration in Fig. 8a reveals a dependence on topography, especially on the territory of Norway.

Similar to the comparison of geoidal surfaces, we also perform a GOCE-internal comparison, with GOCO01S acting as reference. In Tab. 5, statistics of differences between gravity anomalies evaluated from GOCE_DIR, GOCE_SPW and GOCE_TIM with respect to GOCO01S model are given. The smallest standard deviation of 0.870mGal can again be observed in case of GOCE_TIM (same approach as used for determination of GOCO01S). For GOCE_DIR and GOCE_SPW, the standard deviation is approximately twice as big slightly exceeding the value of 1.7mGal. In Fig. 9, the differences are graphically illustrated. Based on the statement we mentioned above, we observe the same pattern as shown in Fig. 6.

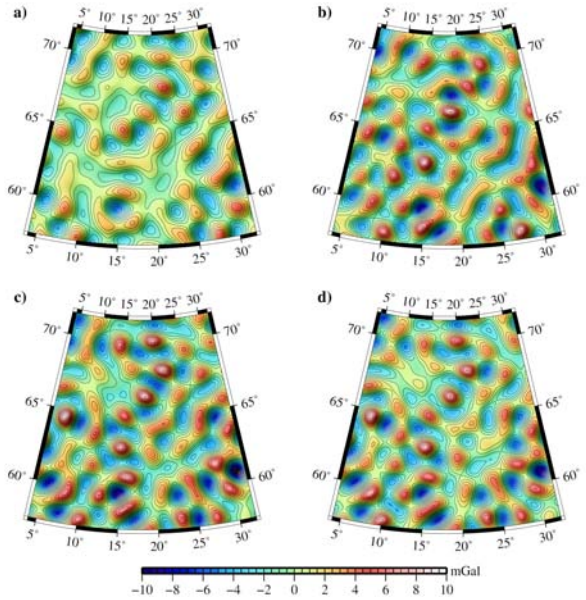

Figure 7: Comparison of gravity anomalies computed by the GOCE derived GGMs with respect to EGM2008: a) GOCE_DIR, b) GOCE_SPW, c) GOCE_TIM, d) GOCO01S

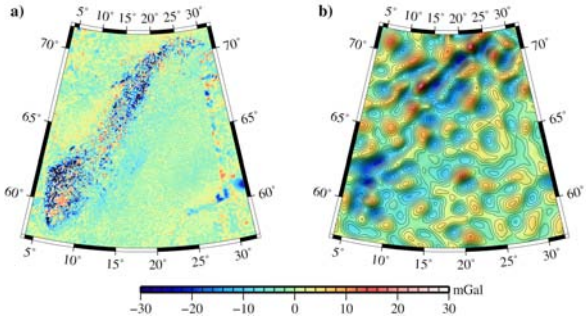

Figure 8: Comparison of the terrestrial mean free-air gravity anomalies with respect to EGM2008: a) Removing of high-frequencies by EGM2008, b) Low-pass filtering in frequency domain

Table 4: Statistics of differences between gravity anomalies with respect to EGM2008 (high frequency part of the terrestrial mean free-air gravity anomalies is removed by EGM2008)

Model	GOCE_DIR	GOCE_SPW	GOCE_TIM	GOCO01S	Terrestrial
Min. (mGal)	-5.988	-9.456	-10.997	-9.873	-108.417
Max. (mGal)	5.052	8.133	9.256	8.370	62.773
Mean. (mGal)	-0.063	-0.039	-0.075	-0.072	-1.756
Std. dev. (mGal)	1.694	2.572	2.778	2.570	7.977

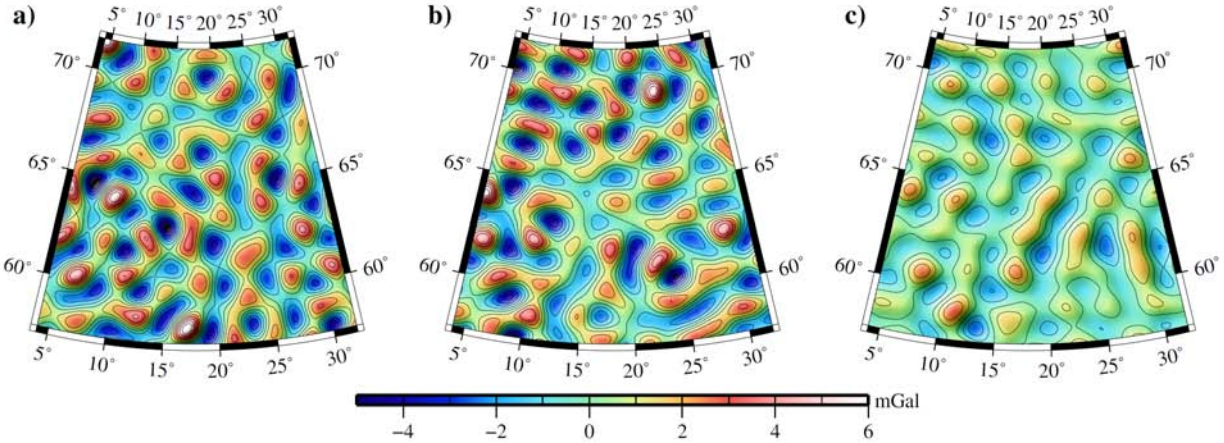

Figure 9: Comparison of gravity anomalies computed by the GOCE derived GGMs with respect to GOCO01S: a) GOCE_DIR, b) GOCE_SPW, c) GOCE_TIM

In the last numerical experiment, gravity anomalies have been low-pass filtered in the frequency domain. All frequencies below 100km have been excluded. To transform the gravity anomalies to the frequency domain and then back to the spatial domain, FFT and its inverse have been performed. In Tab. 6, statistics of differences between low-pass filtered gravity anomalies can be found. Note that EGM2008 low-pass filtered gravity anomalies have been chosen as a reference. It is evident that compared to Tab. 4, minimum and maximum values are reduced. Similarly, standard deviation decrease for the GOCE derived models for several tenths of mGals. The smallest standard deviation can be observed for GOCE_DIR while the largest value shows up in case of GOCE_TIM. Applying our low-pass filtering procedure for the terrestrial mean gravity anomalies, minimum and maximum values are significantly reduced. Also the graphical illustration in Fig. 8b shows a significant smoothing of the differences. However, compared to the GOCE derived models, standard deviations are approximately three times larger. We may suppose that the accuracy of our low-pass filtering procedure is on the level of a few mGal. By comparing Figs. 5b and 8b we can see a similar behavior of differences for the OCTAS geoid and terrestrial mean free-air gravity anomalies. Therefore we conclude that the filtering procedure is realistic even if its accuracy is on the level of few centimeters or mGal respectively.

Table 5: Statistics of differences between gravity anomalies with respect to GOCO01S

Model	GOCE_DIR	GOCE_SPW	GOCE_TIM
Min. (mGal)	-6.037	-5.530	-2.590
Max. (mGal)	6.870	6.431	2.806
Mean. (mGal)	0.010	0.033	-0.002
Std. dev. (mGal)	1.767	1.736	0.870

Table 6: Statistics of differences between gravity anomalies with respect to EGM2008 (gravity anomalies filtered in frequency domain)

Model	GOCE_DIR	GOCE_SPW	GOCE_TIM	GOCO01S	Terrestrial
Min. (mGal)	-4.754	-7.221	-8.291	-7.408	-24.622
Max. (mGal)	4.219	6.034	7.092	6.350	17.844
Mean. (mGal)	-0.053	-0.035	-0.063	-0.061	-1.723
Std. dev. (mGal)	1.395	1.954	2.133	1.947	5.418

5. CONCLUSIONS

In this study, GOCE derived satellite-only GGMs have been compared with EGM2008, the OCTAS geoid and terrestrial gravity anomalies. Numerical experiments have been performed on the territory bounding the continental part of Norway and most of Fennoscandia. Spherical harmonic expansions have been truncated at maximum degree and order 200 corresponding to a spatial resolution of 100km. Higher frequencies of the OCTAS geoid and of the terrestrial gravity anomalies have been removed by either subtracting the signals computed from EGM2008 above degree 200 or by a low-pass Butterworth filter in the frequency domain.

Our numerical experiment shows that the relative differences between geoidal surfaces from GOCE derived GGMs may reach some few decimeters at the spatial resolution of 100km with standard deviations in the range of 6 to 10 cm. This fits nicely to the cumulative errors computed from the formal error standard deviations of the models (which implies, that the errors are correctly calibrated). In the case of gravity anomalies, relative differences may reach several mGal. The smallest standard deviation is observed for GOCE_DIR. We suppose that this is due to the fact, that a-priori information on the gravity field was used for the determination of GOCE_DIR. On the other hand, the largest standard deviations have been obtained when using GOCE_TIM. This model does not contain any a-priori information. The combination model GOCO01S gives the same accuracy at a spatial resolution of 100km as the pure GOCE-derived models.

The numerical experiment demonstrates significant difference of the OCTAS geoid model and the terrestrial mean free-air gravity anomalies. We suppose that these differences are partly caused by the filtering procedures we suggested. Filtering by EGM2008 does not remove all frequencies above degree and order 2190, but only the differences between the models. In this frequency spectrum, one can expect contributions of a few centimeter in terms of geoid heights and of a few mGal in terms of gravity anomalies. On the other hand, by FFT and low-pass filtering in the frequency domain we are able to remove all high frequencies. The precision of this filtering procedure is also on the level of some few centimeter and some few mGal. In future experiments, we will try to improve the filter characteristics, such that the computational errors stay below the level of mm. In addition one might also apply the filter to residual quantities after removing the high frequencies from EGM2008. This should lead to a more consistent approach for the comparison of terrestrial gravity data with GGMs.

Acknowledgements

The study is part of UMB's Nova-GOCE project supported by the Norwegian Research Council under project number 197635 and is carried out in the framework of UMB's ESA-category-1 project 4294 Application and Validation of GOCE and remote sensing data with focus on Northern latitudes. The Norwegian Mapping Authority is highly appreciated for providing terrestrial gravity data and the geoid model over Norway.

REFERENCES

1. Bruinsma S.L., Marty J.C., Balmino G., Biancale R., Foerste C., Abrikosov O., Neumayer H. (2010). GOCE Gravity Field Recovery by Means of the Direct Numerical Method. Proceedings of the ESA Living Planet Symposium, 28 June - 2 July 2010, Bergen, Norway.

2. ESA (1999). Gravity Field and Steady-State Ocean Circulation Mission. Reports for Mission Selection; the Four Candidate Earth Explorer Core Missions. ESA SP-1233(1).

3. Koop R., Visser P., Tscherning C.C. (2001). Aspects of GOCE Calibration. Proceedings of the International GOCE User Workshop, vol. WPP-188, ESA/ESTEC, Noordwijk, Nederlands, pp. 51-56.

4. Migliaccio F., Reguzzoni M., Sansó F., Tscherning C.C., Veicherts M. (2010). GOCE Data Analysis: the Space-Wise Approach and the First Space-Wise Gravity Field Model. Proceedings of the ESA Living Planet Symposium, 28 June - 2 July 2010, Bergen, Norway.

5. Omang O.C.D., Hunegnaw A., Solheim D., Lysaker D.I., Ghazavi K., Nahavandchi H. (2008). Updated OCTAS Geoid in the Northern North Atlantic – OCTAS07. In: Sideris M.G. (Ed.) Observing our Changing Earth, IAG Symposia, vol. 133, Springer, pp 397-403.

6. Pail R., Goiginger H., Mayrhofer R., Schuh W.D., Brockmann J.M., Krasbutter I., Hoeck E., Fecher T. (2010). GOCE Gravity Field Model Derived from Orbit and Gradiometry Data Applying the Time-Wise Method. Proceedings of the ESA Living Planet Symposium, 28 June - 2 July 2010, Bergen, Norway.

7. Pail R., Goiginger H., Schuh W.D., Höck E., Brockmann J.M., Fecher T., Gruber T., Mayer-Gürr T., Kusche J., Jäggi A., Rieser D. (2010). Combined Satellite Gravity Field Model GOCO01S Derived from GOCE and GRACE. Geophysical Research Letters, 37, L20314, doi:10.1029/2010GL044906.

8. Pavlis N.K., Holmes S.A., Kenyon S.C., Factor J.K. (2008). An Earth Gravitational Model to Degree 2160: EGM2008 (2008) General Assembly of the European Geosciences Union, 13–18 April 2008, Vienna, Austria.